CHARACTERIZATION AND HOT CORROSION BEHAVIOR OF BOILER TUBE STEELS AT 700ºC

By

LILIOSA-EYANG ENGONGA OBONO

15763

Dissertation submitted to the Department of Petroleum Engineering
In Partial Fulfillment of the Requirements
For the Degree
Bachelor of Engineering (Hons)
(Petroleum)
September 2014

Universiti Teknologi PETRONAS
Bandar Seri Iskandar
31750 Tronoh
Perak Darul Ridzuan

CERTIFICATION OF APPROVAL

CHARACTERIZATION AND HOT CORROSION BEHAVIOR OF BOILER TUBE STEELS AT 700ºC

By

LILIOSA-EYANG ENGONGA OBONO

15763

A project dissertation submitted to the
Department of Petroleum Engineering
In Partial Fulfillment of the Requirements
For the Degree
Bachelor of Engineering (Hons)
(Petroleum)
September 2014

Approved by,

____

Dr. Subhash Kamal

UNIVERSITI TEKNOLOGI PETRONAS

TRONOH, PERAK

September 2014

CERTIFICATION OF ORIGINALITY

This is to certify that I am responsible for the work submitted in this project, that the original work is my own except as specified in the references and acknowledgements, and that the original work contained herein have not been undertaken or done by unspecified sources or persons.

Liliosa Eyang Engonga Obono

ABSTRACT

Industrial boiler tubes undergo the effect of hot corrosion during their operating lifetime. The main objective of this project is, to study the degree of hot corrosion affection to the base steel metal, used in the manufacturing of boiler tubes.

The objective is attained by initially characterizing, and quantifying the chemical composition of the alloy in question, on both surface and cross-sectional areas.

Continuously, the alloy samples are exposed to a corrosive environment, composed basically of molten salts: sodium sulphate (Na_2SO_4) and sodium chloride (NaCl), in a laboratory oven at a temperature of 700^oC.

This is done to subject the metal to the effect of hot corrosion.

Once the samples have undergone oxidation and hot corrosion, Scanning Electron Microscope (SEM) analysis is done to study the surface morphology, and identify the chemical composition present after the process.

The degree of penetration of the hot corrosion, through the cross section of the sample is also analyzed, to determine how deep the hot corrosion is able to penetrate the sample, during the total number of cycles applied in the experiment.

ACKNOWLEDGEMENT

I would like to express my sincere appreciation to Dr. Subhash Kamal, my project supervisor, for all the time dedicated to coaching, advising, and supporting, during the entire realization of my Final Year Project. For giving me the opportunity to involve myself in a purely Mechanical Engineering Project, and the trust to my potential despite me being a Petroleum Engineering Student.

Thank you Bezawit, my last 2 years life companion, for being an unconditional support during all the difficult periods faced.

To GC, for the emotional support, and for the incredible way of always being present, from that far. Thank you for being here exactly when I needed you to.

I dedicate this project to Angela Eyang, for cheering this last period of university life, and thus this FYP project, through the eagerness of meeting her soon. To Ana-Lourdes and Alejandro.

To God, for making it ALL possible.

L.

TABLE OF CONTENTS

LIST OF FIGURES

LIST OF TABLES

CHAPTER 1

INTRODUCTION

1.1 BACKGROUND OF THE STUDY

The human industrial era is characterized by engineering systems that operate at high temperatures. Uncountable systems could be pointed out, from the residential boilers used to heat water for home use, to the most sophisticated space-crafts.

This project is focused on the boiling systems of thermal power plants. In this type of plants, power is generated through boiling and subsequence condensation of water, based on the principle of the Rankine cycle.

Superheated steam is generated in the boiler, under pressure; the steam drives a steam turbine, which is connected to a power generator. The steam is circulated to its condensation phase through a cooling tower; the water is then pumped back to the boiler for steam re-generation. (Kapooria et. al 2008).

Fuel, in the form of carbon or gas is burned to run the boiler. The resulting combustion gases are used to achieve water vaporization. The type of boiler used for this application is mostly a pressure vessel containing an array of internal tubes. The water is circulated inside the tubes, while the combustion gases surround the tubes; the steam generation is achieved through the heat exchange between the combustion gases, and the water contained inside the tubes.

Although thermal boilers are generally designed for a long term operation, the continuous exposure of its internal tubes to the corrosive environment leads to hot corrosion. The base metal experiences an accelerated oxidation, due to a layer of molten salts over the surface, created by the hot combustion gases. These hot gases react with the components of the boiler tube steel, resulting in the destruction of the mechanical and thermal properties of the tubes. (Ravindra et. al 2007).

Consequently, the boiler tube steel gets disintegrated, and it can easily be fractured or fragmented into small solid pieces. This problem ultimately affects the boiler efficiency, cost, and also has a high impact on the life time and the reliability of thermal boilers.

1.2 PROBLEM STATEMENT

The thermal boilers' continuous exposure to high temperatures (in the range of 600^oC to 1200^oC), and a corrosive environment, gives rise to the necessity of studying better ways of improving the thermal and corrosion resistance of the super alloys, which the boiler tubes are made of.

Failure of the boiler tube mechanical structure, due to high temperature corrosion affects the performance of the boiler, and consequently the overall efficiency of the power generation system. Moreover, the lifetime and the reliability of the boiler is compromised, and thus the boiler manufacturers need to ensure that, the boiler steel meets the necessary thermal and mechanical requirements, for the specific process for which the boiler is purchased, as well as the expected life time.

1.3 OBJECTIVES

The objectives of this project are listed as follows:

- Characterize the chemical composition of the boiler tube steels KHR35C.
- Analyze the hot corrosion behavior of boiler tube steel, after exposure to a temperature of 700^oC.
- Determine the degree of hot corrosion penetration, through the surface of the steel sample, and identify the main corrosion-contributing elements.

1.4 SCOPE OF STUDY

The scope of this project encloses the analysis of the reaction of boiler tube steels, to the corrosive environment generated by the combustion gases (oxidizing gas atmosphere) and molten salts; and the identification of the most relevant alloy elements, contributing to the high temperature corrosion.

The objectives of the project can be achieved within two semesters, since the main difficulties lay on the acquisition of the steel samples, and the simulation of the corrosive environment, in an actual incineration plant.

All other equipment necessary to complete the project can be found in the UTP laboratories.
Due to the unavailability of an incineration plant, the experiments were done using a laboratory furnace, and a corrosive environment created with molten sodium sulphate and sodium chloride.

1.5 RELEVANCY AND FEASIBILITY OF THE PROJECT

One of the main consequences of the effect of hot corrosion on boiler tube steels, is the erosion of the corrosion products, and further fragmentation of these into small solids. These solids are transported downstream into the turbine system, and erode turbine valves, fan, and other components. The obvious outcome of this event is the shortening of the useful lifetime of the turbine.

This project becomes relevant because the elements which are more corrosion-contributing will be identified, such that the manufacturers will modify the steel manufacturing process, either by reducing the quantity of these elements, or by adding effective substitutes to them. One common remedy of the hot corrosion effect is the coating of the steel, using thermal spray coatings.

The feasibility of the project relies on the fact that, most of the equipment necessary to complete the project can be found in the UTP laboratories, and thus the time allocated to complete the project (2 semesters), is reasonable enough to accomplish its objectives.

CHAPTER 2
LITERATURE REVIEW

2.1 OXIDATION AND HOT CORROSION OF SUPER-ALLOYS

Metallic super-alloys compose the main structural parts of any engineering system, operating at high temperatures, of about 600°C and above. Super-alloys are a combination of several metallic elements, manufactured in order to obtain a steel material, which is able to fulfill the requirement of severe mechanical stress and temperature resistance, under specific operating conditions. (Pollock & Tin, 2006).

Oxidation occurs due to the alloy being composed of different metals, which may react with oxygen in a high temperature, and corrosive environment. Hot corrosion occurs as a result of the oxidation, and the spallation of the metallic oxides.

According to Stringer (1993), materials for high temperature applications, must be manufactured such that, they comply with the required engineering function cost-effectively. The issues faced by the super-alloys operating at high temperatures can be divided into oxidation and exfoliation.

2.1.1 Oxidation of Alloys

The metallic alloy elements are treated so that, resistance to oxidation is developed through a process called selective oxidation. Selective oxidation consists on a specific element of the oxide being oxidized, forming a layer over the substrate metal. This oxide layer serves as the metal protective layer.

In order for this process to take place, sufficient quantity of the oxidizing element must be present, and this reaction must take place at very slow rates.

Aluminum (Al), chromium (Cr) and silicon (Si) are the only elements in nature, complying with the above requirements. Their oxides (Alumina Al_2O_3, and Chromia Cr_2O_3) provide sufficient protection, and their affinity to oxygen is high enough for selective oxidation to occur. (Meier & Pettit 1999).

Nevertheless, the high operating temperatures to which the alloy is subjected, turn silicon into a non-feasible element for this purpose. Thus, the nickel-cobalt- and iron- base super-alloys utilize aluminum and chromium to build a protective oxide layer, and cover the substrate from oxidation degradation.

These authors also outline the factors affecting selective oxidation, which are:

- The alloy’s composition.
- The alloy’s surface conditions.
- The corrosive gas environment.
- Cracking of the oxide scale.

After the protective oxide has been formed, another type of oxidation occurs, whereby this oxide layer is destroyed through cracking and spallation. This is known as cyclic oxidation, and it occurs basically due to the contact with the gaseous corrosive environment.

Additionally, the thermal cycles undergone by the equipment upon cooling can lead to the generation of cracks on the protective oxide, after various turn on and shut down cycles.

2.1.2 Exfoliation

The exfoliation of the alloy protective oxide consists in the disintegration of solid particles on the metal’s surface. Stringer (1993) discusses two main issues as a result of this process. The first one compromises the lifetime of the equipment, (in this research, the boiler), and is the fact that several cycles of exfoliation and regeneration of the protective layer, ultimately lead to the depletion of the element undergoing selective oxidation; therefore, at some stage of the boiler’s life cycle, there will be no protective oxide on the substrate.

The second issue is regarded to the boilers, where the oxide exfoliation occurs on the inside of the super-heater and re-heater tubing and piping systems; the oxide fragments are carried further through the steam stream, and erode the steam valves and other turbine components downstream.

The exfoliation process may occur due to different reasons, some of them pointed below:

-The mechanical stresses resulting from the thermal cycles may cause adhesive failure between the protective oxide layer and the substrate, and/or cohesive failure in either of them.

-The elastic strain of the metallic alloy may be greater than the fracture strain of the oxide-metal interface. And thus, this interface may fail while the alloy itself still conserves its mechanical properties.

-Voids resulting from the protective layer growth may be formed in the interface, between the oxide and the substrate.

2.1.3 Molten salt accelerated oxidation

The composition of the super-alloy operating in a highly corrosive environment may lead to the formation of salt solutions, which contribute to the destruction of the protective oxide layer, and accelerate the corrosion of the metal. Stringer (1993) mentions some molten salt species such as V_2O_5, Na_2SO_4, and PbO_2, and explains the occurrence of this type of oxidation, in two ways:

The first method consists in the molten salt being diffused, into the oxide-metal substrate interface; this way the oxide layer is weakened, and becomes more prompt to exfoliation. Another way molten salts affect the protective oxide is by dissolving it. Once the protective oxide scale has been destroyed in either way, hot corrosion accelerates.

Kamal & Prakash (2010) also outline the presence of molten salt solutions in energy generation systems. The Na_2SO_4 can be a result of a reaction between NaCl and sulphur impurities. The V_2O_5 on the other hand is a combustion product of vanadium porphyrin present in oil and fossil fuels.

2.2 REMEDIES OF HOT CORROSION: THERMAL SPRAY COATINGS

Thermal spray coatings are processes applied to a vast number of metallic components to enhance their structural integrity, and protect them from oxidation, wear, etc.

According to Kamal et. al (2012), this type of coatings play a vital role in the protection of turbine engines from oxidation and hot corrosion.

There are various ways in which thermal coatings can be carried on, but this topic focuses on the flame spray coating, used to coat steel.

According to TST (Thermal Spray Technologies), thermal spray coatings consist of processes where heat is used to melt a coating material into powder, wire or rod form. This material is then sprayed on a prepared surface, by expanding process gases. It quenches upon impact with the surface and bonds.

This company lists the type of thermal spray coating processes as follows:

- **Plasma-Arc Spray Coating:** The most versatile of all the thermal spray processes. Plasma spray coatings can be employed on all materials considered sprayable.
- **Shrouded Plasma-Arc Spray Coating:** Plasma is sprayed with a shroud of protective gas. The shroud is used to help protect the spray plume from the atmospheric environment.
- **High Velocity Oxy-Fuel Coating (HVOF):** High velocity oxy-fuel coating (HVOF) is a subset of flame spraying. This technology is capable of producing very dense and well adhered coatings in the as-sprayed condition.
- **Electric-Arc Spray Coating:** Electric-arc spray coating uses two conductive wires to carry electrical charges of opposite polarity. When the two charges meet at the front of the spray device an electrical arc is created and this arc melts the wire. The molten wire is the feedstock material for creating a coating. It has the capability of depositing coatings at very high spray rates.
- **Flame Spray Coating:** Flame spray coating employs combustion of gases to melt powder, wire or rod material and propel the molten droplets onto a surface to create a coating. Its gas velocities are much slower than HVOF. Flame spraying

can create coatings out of a wide range of materials from plastics to oxide ceramics.

Cold Spray Coating: Cold spray is the newest member of the thermal spray technologies. Cold spray coating relies on very high gas velocities to propel particles and provide a high degree of kinetic energy. The kinetic energy causes plastic deformation of the particles upon impact, which creates very dense coatings.

2.2.1 Flame Spray Coating

Flame sprays coatings offered by TST use powder, wire, or rod as the spray material. The fuel gases used to achieve melting may include hydrogen, propane, natural gas, acetylene, etc. The combustion takes place in an unconfined manner.

Low temperatures and velocities associated to this type of coating process result in higher oxides, porosity and inclusion in coatings.

Figure 1 is a diagram illustrating a flame spray coating process.

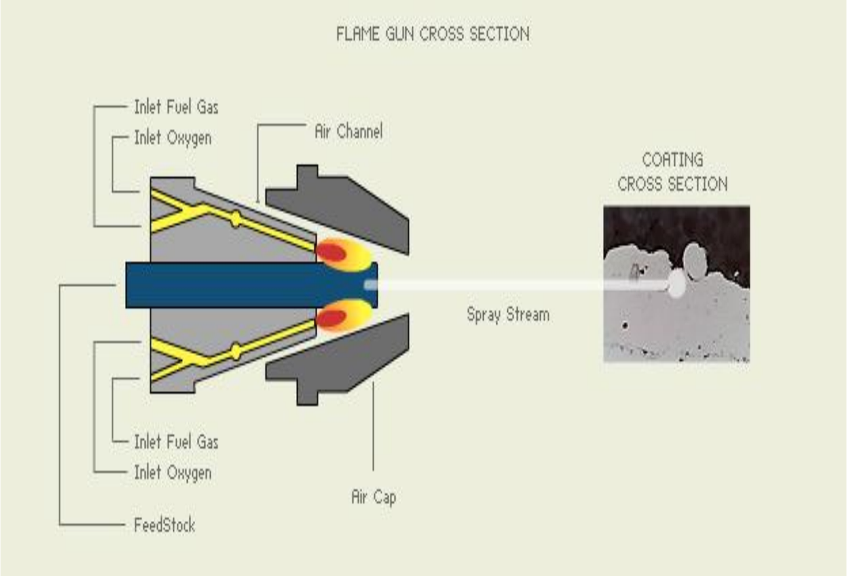

Figure 1. Flame Spray Coating.

Source: Thermal Spray Technologies.

Applications

One of the applications of the flame spray coating is in providing wear and particle impact resistance. It is used for producing spray and fuse coatings.

The wear resistance material is deposited first using flame spraying, and then the coating is deposited. The coating material is designed to have a lower melting point than the base metal on which it will deposit. The fuse between wearing and coating materials then take place, by applying heat in the range between the solid and liquid phases of both materials, for them to fuse. This way most of the porosity in the coating layer is eliminated.

2.2.2 Coating Materials

Generally, any material capable of melting when subjected to a specific range of temperature can be used in a thermal spray process. Some of the thermal spray processes can generate temperatures as high as 16,500^{o}C.

Almost all the metals can be coating materials. Many plastics are also used as coating materials. Materials that sublime can also be used as coating materials, by mixing them with a material that melts, so that the latter acts like cement when both deposit on the substrate.

CHAPTER 3
METHODOLOGY

This chapter describes the project work execution. The process is broken down into consecutive phases, explained in detail in the following sub-topics.

3.1 PROJECT METHODOLOGY

3.1.1 Acquisition of samples

In order to assess the oxidation and hot corrosion resistance of boiler tube steels, these are provided by manufacturers. Seamless steel is the type of steel used in the manufacturing of boiler tubes. A type of nickel based steel material called KHR35C, is used to conduct the experiments of this project.

3.1.2 Preparation of samples

A total of 9 samples have been cut and are to be grinded to achieve horizontal surfaces, since the original steel sample was cylindrical in shape.

The steel samples' dimensions are 15mm x 20mm (L x H) with a variable thickness. The variability in thickness is due to the geometry of the original sample.

3.1.3 Samples tests in the incinerator/furnace

After the chemical composition of the steel has been determined, the samples are placed in the incinerator/furnace, at a temperature range between 600^{o}C to 1200^{o}C. The exposure to heat is to be done in a cyclic pattern, to mimic the harsh operating conditions in which these metals actually operate.

3.1.4 SEM (Scanning Electron Microscope)

The samples are analyzed under the SEM to view the sample surface morphology, and the chemical elements present on it. Appendix I contains a microscopic view of the surface morphologies of the samples tested.

3.1.5 XRD (X-ray Diffraction Analysis) Test

The XRD test is done on each of the samples, after they have been removed from the incinerator, and cooled. This test defines the chemical content of the corrosion product, as well as the degree of penetration of the corrosion, through the sample surface.

3.2 KHR35C STEEL ALLOY SPECIFICATION

The steel specification details are outlined in table 1. Table 2 gives a more detailed chemical composition, including every single chemical element present in the steel in weight percentage.

Table 1. Steel specification

Material	KHR35C
Composition	25Cr - 35Ni - 1Nb
Characteristics and Advantages	-High creep rupture strength by adding Nb to HP (25Cr - 35Ni) alloy. -Grain boundary net-work is finer and much stabilized at high temperature.

Table 2. Steel Chemical Composition

KHR35C		
Chemical Composition (wt%)	C (carbon)	0.4/0.5
	Si (silicon)	1.5 max.
	Mn (manganese)	1.5 max.
	Ni (nickel)	34/37
	Cr (chromium)	24/28
	Nb (niobium)	0.6/1.5

3.3 PROJECT KEY MILESTONES

The project key milestones are presented in figure 2 below.

May-June 2014

Project initiation.

Preliminary research on project topic.

June-July 2014

Literature review/methodology research.

Sample enquiry. Proposal report.

July-Sept 2014

Acquisition of samples.

Interim Report.

Sept-Oct 2014

Acquisition of samples.

Sample analysis/Sample testing

Oct-Nov 2014

Sample analysis. Result Analysis.
Progress Report.

Nov-Dec 2014

Completion of deliverables.

Dissertation report.

Figure 2. Project Key Milestones

3.4 GANTT CHART

Project Event	FYP I (May 2014)				FYP II (May 2014)			
	May	June	July	Aug.	Sep.	Oct.	Nov.	Dec.
Project assignation and introduction to project supervisor.	■							
Initial investigation, background study, literature review and methodology.		■	■					
Sample enquiry to steel manufacturers for texting. Sample acquisition.		■	■	■				
Submission of extended proposal report. Proposal defense.			■					
Submission of Interim report.				■				
Hot corrosion analysis, and sample characterization Sample analysis. Sample testing					■	■	■	
Submission progress report, technical paper, and dissertation report.						■	■	■

Figure 3. Project Gantt Chart

CHAPTER 4

EXPERIMENT

4.1 SAMPLE PREPARATION

A KHR35C steel sheet was provided by the Corrosion Laboratory of Universiti Teknologi Petronas. This steel sheet was cut into nine rectangular samples.

The cylindrical shape of the sheet was transformed into rectangular samples, 15mm x 20mm (L x H) with variable thickness. Figure 4 illustrates the initial physical appearance of the samples.

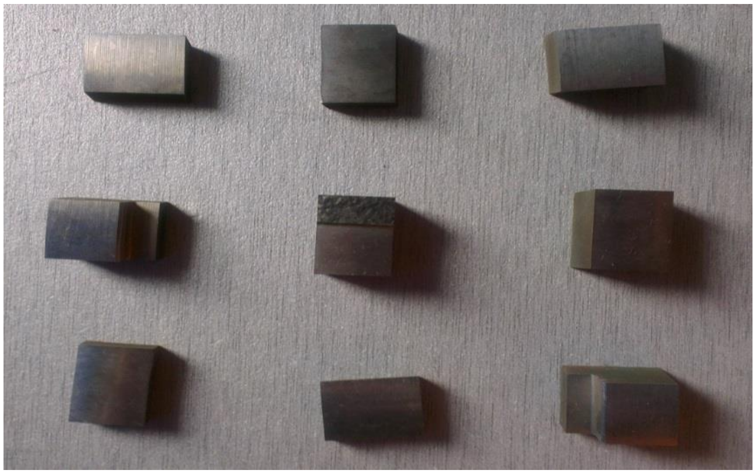

Figure 4. Original physical appearance of steel KHR35C samples

The surfaces in the steel samples illustrated in figure 4 have been flattened, using a grinding machine. This process has led to the thinning of most samples, and the reduction of some of the sizes. Figure 5 is an illustration of the final appearance of the samples. Only the ones presenting the biggest thickness will be used, to test the hot corrosion behavior of this type of steel. The sample with the biggest dimensions in mm^3 is L x H x W (20x15x11).

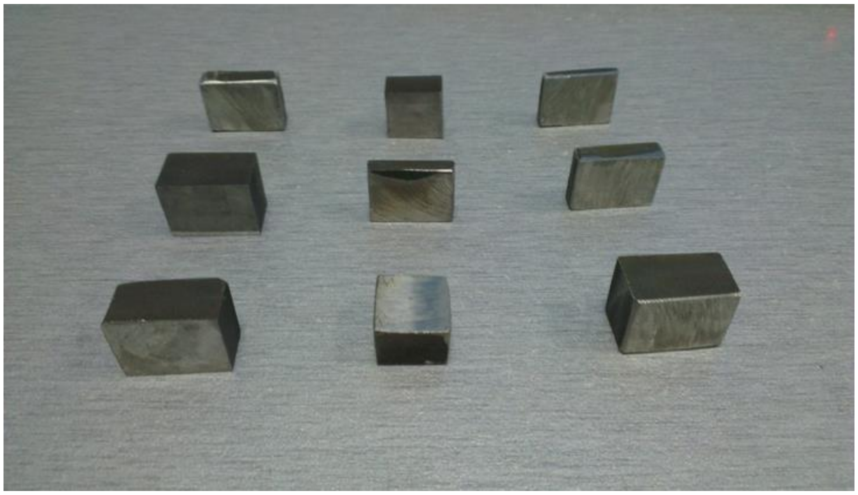

Figure 5. Final physical appearance of steel KHR35C samples.

4.2 ALUMINA CRUCIBLES

The unavailability of any incinerator or nearby thermal power plant, led to the decision of conducting the experiment in a laboratory furnace. For this reason, it was necessary to acquire alumina crucibles, which are ceramic structures in which samples are placed in processes such as melting, fusing, sintering, annealing, burning, incineration and ignition. The alumina crucibles used in this experiment have been purchased from H_2O Generate Sdn. Bhd, a local Malaysian supplier.

Figure 6 constitutes two samples of the acquired alumina crucibles, to be used during the high temperature exposition of the samples. The crucible specifications are stated below:

Alumina Boat Flat Bottom
LxWxH: 85x45x23 mm (outer)
80x40x20 mm (inner)

More than 95% of its composition is Al_2O_3, and they can withstand temperatures up to 1300^{o}C.

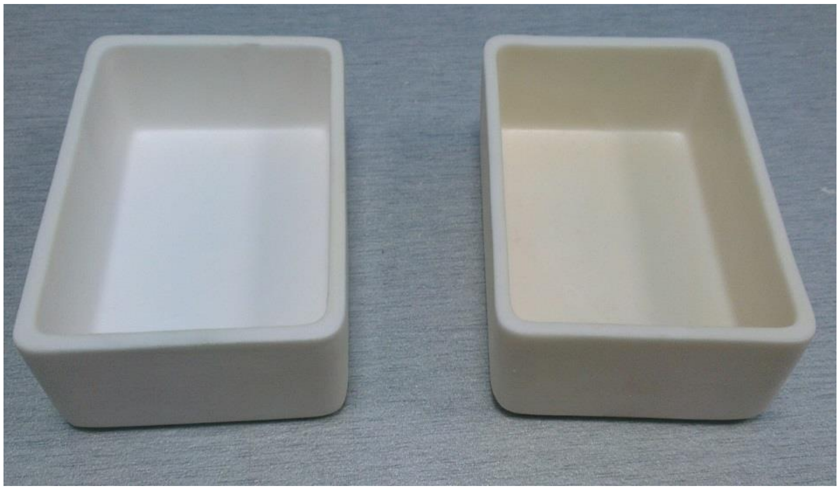

Figure 6. Alumina crucibles

4.3 EXPERIMENT

The experiment was carried on in a laboratory furnace. In this case, a high temperature box furnace was used, to expose the samples to heat at 700°C. This furnace is manufactured by Carbolite.

The experiment was designed to place three samples in the furnace, at the same time. Sample number 1 in air, and samples 2 and 3 coated with salt solutions.

Before exposure, two salt solutions were mixed with distilled water. The first one was sodium sulphate (Na_2SO_4) solution, and the second one was a mixture of sodium sulphate and sodium chloride (Na_2SO_4 + NaCl).

All the samples were heated at 200°C, in an oven. This was done to facilitate the coating of the salt solutions on the samples. After coating, the samples were again placed in the oven for another three minutes, to assure the placement of the solution on the surfaces.

The characteristics of each sample are specified in table 3.

In the operation of boilers, NaCl from seawater reacts with the sulphur impurities found in the fuel, to generate sodium sulphate. (Kamal et. al, 2010) .Therefore the election of salts is realistic since these are commonly present in a real scenario.

The heat exposure was done in 8 cycles, where one cycle consisted of 1 hour exposure in the furnace, following a 15 minutes cooling at a room temperature of 25° C, and weighing.

The process was carried on in cyclic conditions in order to mimic the accelerated environment, in which the super-alloy is exposed in real life processes.

The purpose of weighing the samples is to better characterize the kinetics of oxidation and hot corrosion.

Table 3. Sample description and characteristics.

	SAMPLE		
	1	2	3
Coating	No	Yes	Yes
Solution	Air	Na_2SO_4	Na_2SO_4 + NaCl
Initial weight (g)	24.5	27.55	26.79
Crucible weight (g)	193.15	188.55	193.68
Total weight (g)	217.65	216.10	220.27
Total weight after coating (g)	217.65	216.33	220.76

The experiment was designed to be conducted for a total of 8 continuous cycles. Due to logistic issues the first three cycles were realized first, and the samples were deposited inside a desiccator. The other five cycles were completed the following day.

CHAPTER 5

RESULTS AND DISCUSSION

5.1 EXPERIMENTAL RESULTS

After the first cycle, sample 1 did not experience a significant visual change. Sample 2 presented the dried salt solution which had turned white on its surface, while sample 3 had turned into a black shedding color, while portions of salt had started turning green in its surroundings, (see figure 7).

Figure 7. Left to right. Sample 1, 2 and 3 after the first cycle.

Figure 8 presents the samples after the second cycle. Sample 1 experienced a changed from grey to a reddish color, while the dried salt solution on sample 2 started turning into a greenish color; sample 3 continued to get darker with a cap made of particles on the surface.

At the end of the experiment, and after the three samples had undergone the eight cycles whereby, sample 1 was oxidized, and samples 2 and 3 were corroded under different aggressive conditions, sample 1 presented a reddish color, the green color resulting from the sodium sulphate reaction was clearly visualized on the surface of the sample 2. Finally sample 3 presented a black surface, but green tiny particles could also be appreciated; this sample left corrosion products in the crucible, (figure 9).

Figure 8. Left to right. Sample 1, 2 and 3 after the second cycle.

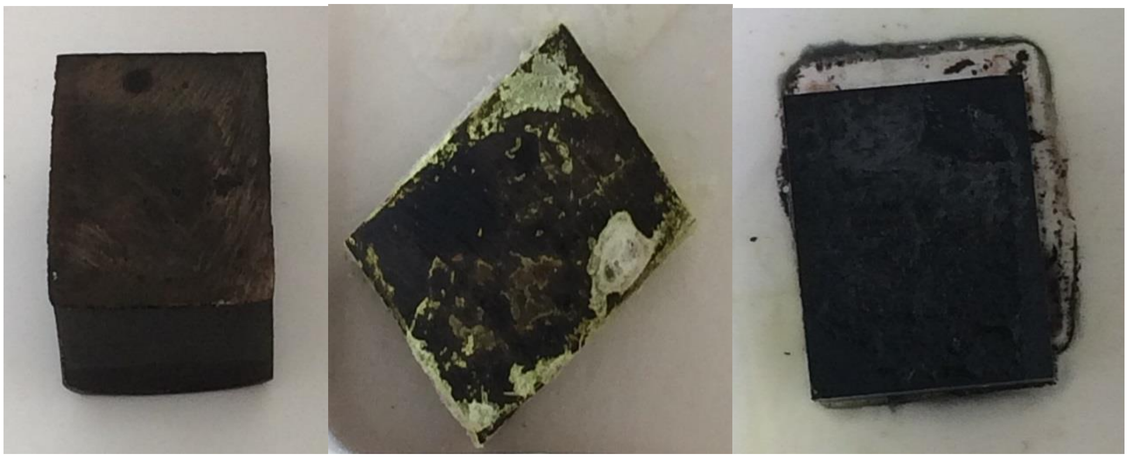

Figure 9. Left to right. Sample 1, 2 and 3 after the last cycle.

5.2 WEIGHT CHANGE OF SAMPLES

All the weight measurements (in grams) presented in this section, were done to characterize the kinetics of the oxidation of sample 1, and hot corrosion in samples 2 and 3. These measurements were taken at the end of each cycle, after the cooling process, using an electronic balance.

In table 4 the total weight corresponds to the sample with the crucible, while the effective weight corresponds to the total weight minus the weight of the crucible. The terms weight in and weight out are the measurements before and after the cycle, respectively. The effective weight variation represents the change of weight of the sample due to oxidation and corrosion.

Table 4. Experimental sample weight measurements.

		TOTAL WEIGHT		EFFECTIVE WEIGHT	
	Sample	Weight-in (g)	Weight-out (g)	Weight-in (g)	Weight-out (g)
CYCLE 1	1	217.65	217.62	24.5	24.47
	2	216.33	216.32	27.78	27.77
	3	220.76	220.78	27.08	27.1
CYCLE 2	1	217.59	217.59	24.44	24.44
	2	216.27	216.27	27.72	27.72
	3	220.75	220.75	27.07	27.07
CYCLE 3	1	217.59	217.62	24.44	24.47
	2	216.27	216.30	27.72	27.75
	3	220.75	220.78	27.07	27.1
CYCLE 4	1	217.62	217.63	24.47	24.48
	2	216.30	216.31	27.75	27.76
	3	220.78	220.79	27.1	27.11
CYCLE 5	1	217.63	217.63	24.48	24.48
	2	216.31	216.31	27.76	27.76
	3	220.79	220.79	27.11	27.11

CYCLE 6	1	217.63	217.63	24.48	24.48
	2	216.31	216.31	27.76	27.76
	3	220.79	220.76	27.11	27.08
CYCLE 7	1	217.63	217.62	24.48	24.47
	2	216.31	216.31	27.76	27.76
	3	220.76	220.73	27.08	27.05
CYCLE 8	1	217.62	217.62	24.47	24.47
	2	216.31	216.31	27.76	27.76
	3	220.73	220.70	27.05	27.02

The data gathered in table 4 above is graphically represented in figure 10.

Sample 1 (oxidation in air) experiences a slight decrease in weight after the first cycle, from the second to the third cycle the weight increases again and as from the fourth cycle, the weight varies slightly by 10 mg.

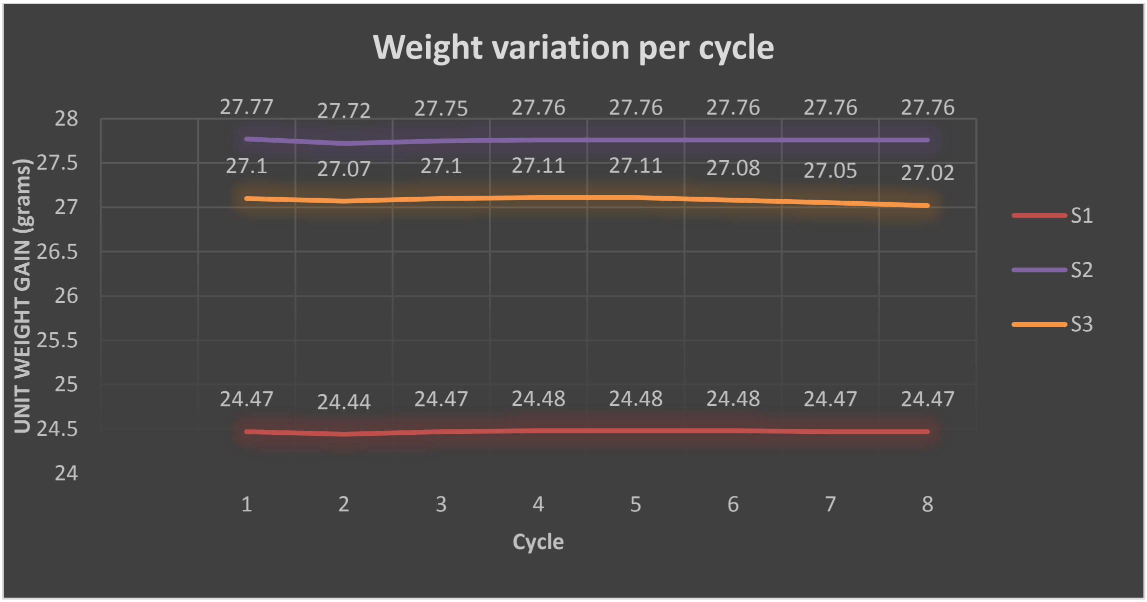

Figure 10. Sample weight variation per cycle

All the sample experience a decrease in weight during the first 2 cycles because any moisture present on them was dried, before any oxidation and hot corrosion process started. The further increase in weight is attributed to the formation of the protective oxide layer, over the substrate, as a result of the diffusion of the elements in question.

The weight in the last cycles remains relatively constant since the protective oxide layer has been formed, and there is no more selective oxidation going on.

Sample 3 on its own, experiences a decrease in weight during the last cycles. This is due to the destruction of the protective oxide layer, as well as the disintegration of the corrosion products, which in fact have been visualized in the crucible.

Figure 11 shows the weight gain per each sample over the number of cycles. Constant intervals represent processes where there was no weight gain registered.

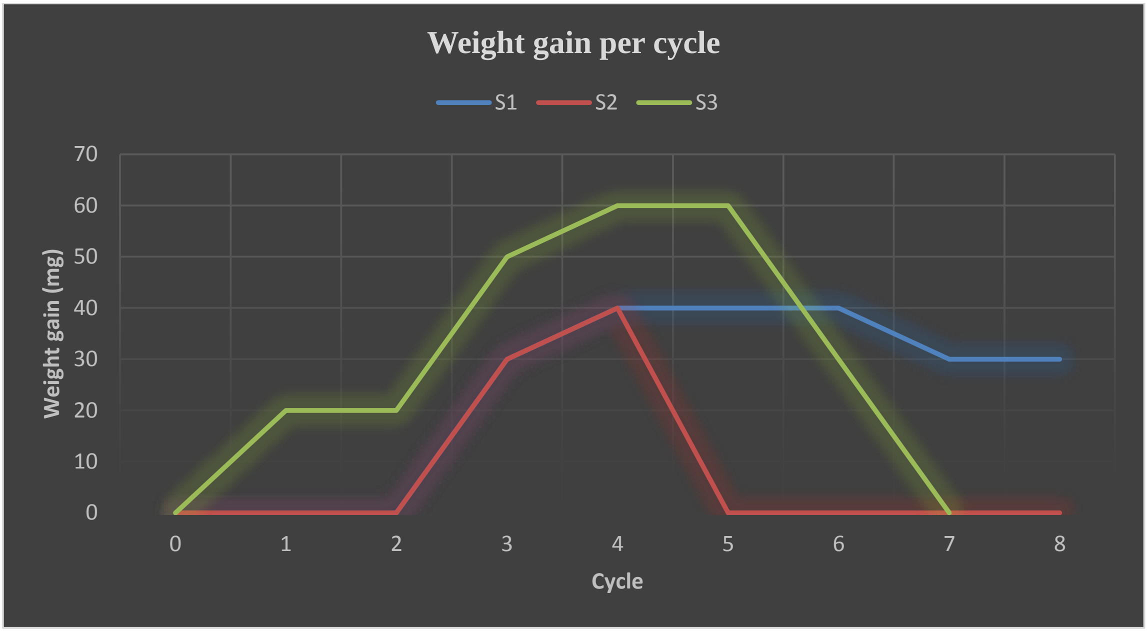

Figure 11. Weight gain per cycle

Figure 12 is an illustration of the difference between the weight of samples before and after the experiment. It is seen that sample 1 had a minimal variation of 10 mg, while samples 2 and three had variations of 30 mg and 60 mg, respectively.

It is reasonable to have this trends since samples 2 and 3 were coated with salt solution; however, the hot corrosion taking is highly attributable to this weight, since as it will be seen in the next section, micro-crystals formed on sample 2.

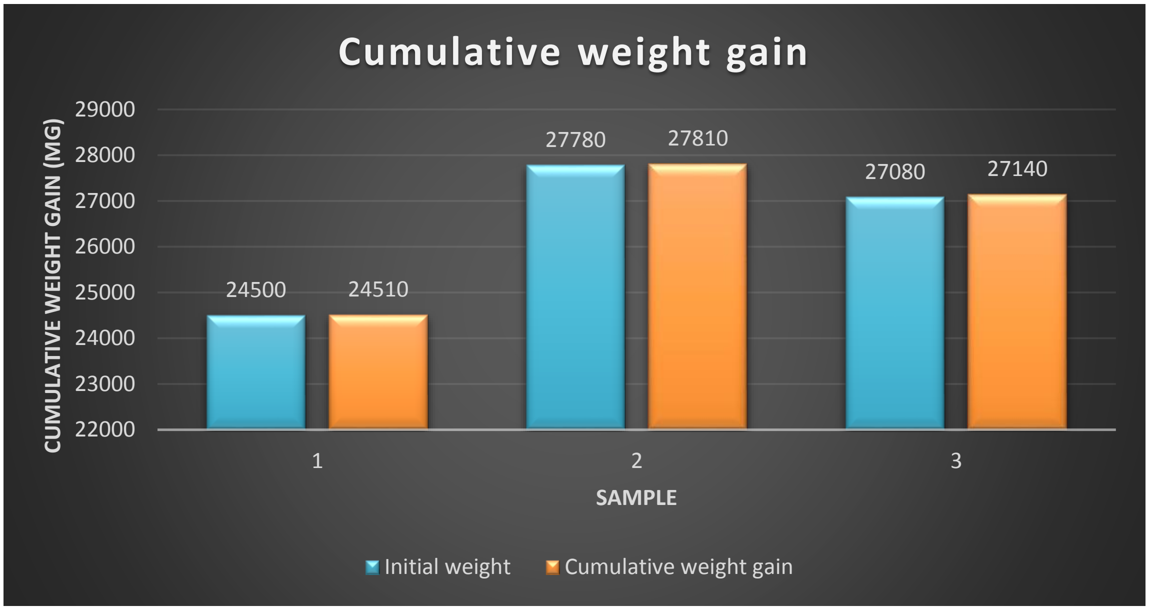

Figure 12. Cumulative weight gain

5.3 SCANNING ELECTRON MICROSCOPE (SEM)/ ENERGY-DISPERSED SPECTROSCOPY (EDS) ANALYSIS.

This section describes the results obtained from reading the samples under the SEM (Scanning Electron Microscope). The surface morphologies of the samples were viewed, and an EDS (Energy-Dispersed Spectroscopy) techniques was used to characterize the chemical composition of the sample surfaces.

For the purposes of the analysis of results, four samples were analyzed under these techniques. The sample description is as follows:

- Sample 0: This is an original KHR35C sample as per figure 5. This sample has not been exposed to neither an oxidation, nor a hot corrosion environment.
- Sample 1: This is the sample exposed to cyclic oxidation in air.
- Sample 2: This is the sample exposed to hot corrosion in the presence of sodium sulphate salt solution.
- Sample 3: This is the sample exposed to hot corrosion in the presence of sodium sulphate and sodium chloride salt solutions.

5.3.1 Sample 0. SEM and EDS.

Sample 0 showed the scratches on the surface as a result of the grinding process, when the surfaces were being flattened. Figure 10 a) shows the sample without magnification, while figure 10 b) shows the sample surface with a magnification of 500X and a spatial resolution of 536µm.

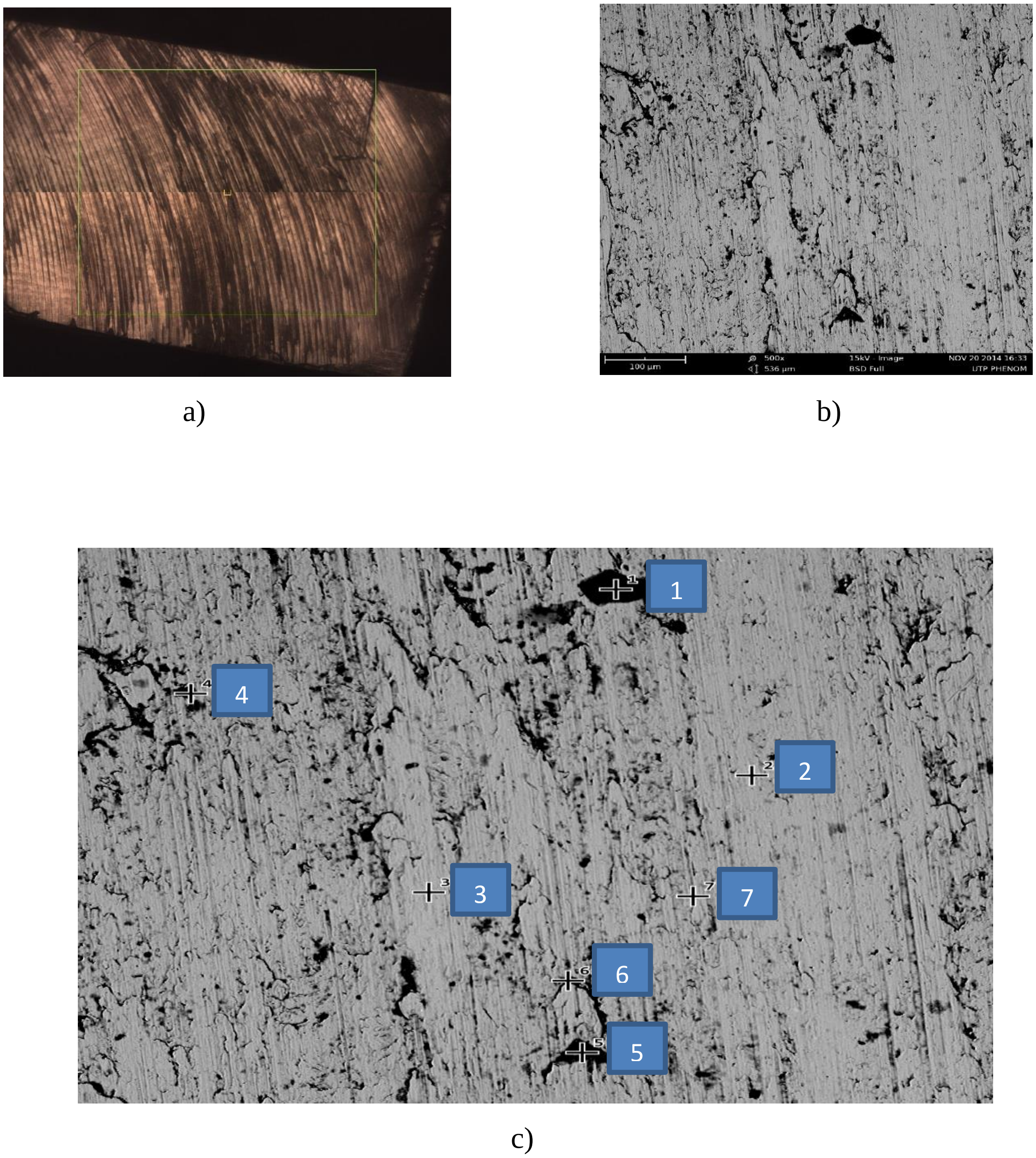

a)

b)

c)

Figure 13. Sample 0, surface morphology.

Figure 13 c) constitutes the surface morphology of sample 0, over which certain spots of interest have been chosen randomly, to characterize the chemical composition. It is useful to point out that the SEM is not 100% accurate, nonetheless table 5 contains the chemical composition present in each spot.

Table 5. Chemical composition. Sample 0.

Element	**Concentration**						
	Spot 1	**Spot 2**	**Spot 3**	**Spot 4**	**Spot 5**	**Spot 6**	**Spot 7**
Carbon (C)	9.5	1.9	1.7	3	7.2	13.8	1.4
Iron (Fe)	21.4	38.4	37	31.7	20	3.9	32
Chromium (Cr)	13.8	22.2	21.6	19.4	12.1	2.4	17.8
Oxygen (O)	22.8			17.6	18.7	53.2	18.2
Nickel (Ni)	16.6	32.4	31	25.1	15.8		26.1
Nitrogen (N)	6.8					5.8	
Silicon (Si)	2.0	5.1	5.4	3.3	2.9	1.2	4.5
Sodium (Na)	5.5				14.4	12.5	
Niobium (Nb)			3.3				
Chlorine (Cl)	1.5				3.2	2	
Potassium (K)						1.7	
Molybdenum (Mo)						2	
Alluminium (Al)						1.4	
TOTAL	**99.9**	**100**	**100**	**100**	**94.3**	**99.9**	**100**

5.3.2 Sample 1. SEM and EDS.

Sample 1 reveals a spallation process as a result of the cyclic oxidation in air, taken place during the exposure to heat in the furnace (figure 14). Similarly to sample 0, specific spots were randomly chosen to run an EDS, and characterize the chemical composition, visualized in table 6.

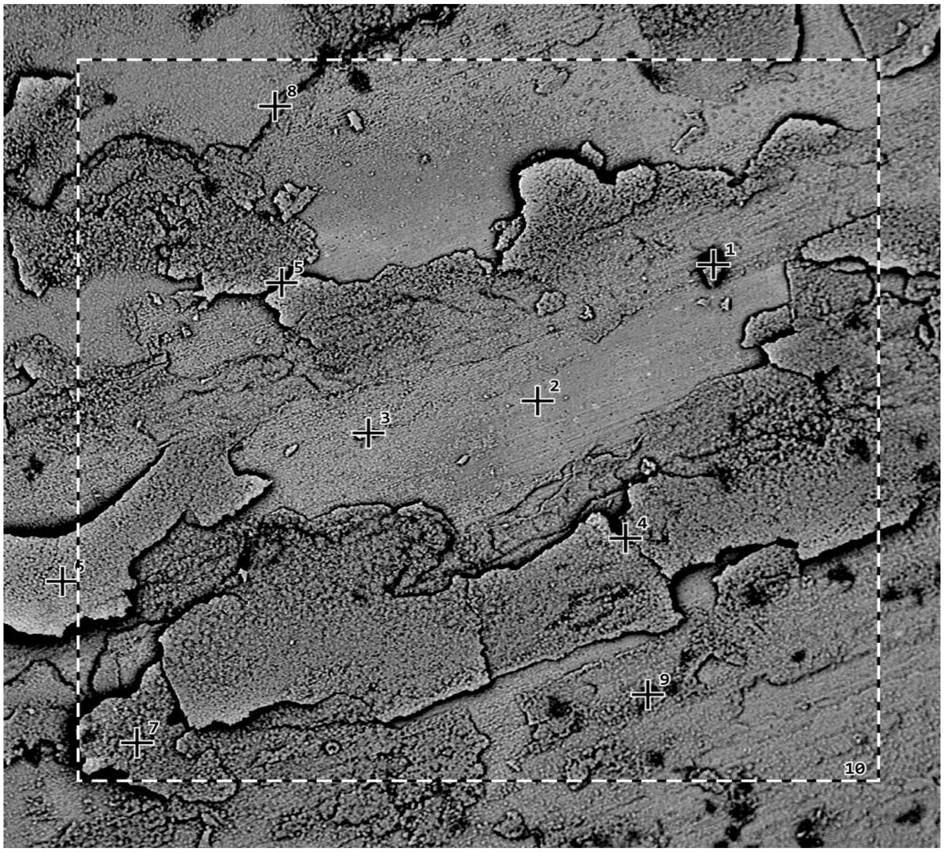

Figure 14. Sample 1, surface morphology.

The fragmented layers observed in the figure above, would detach from the metallic substrate, after long periods of exposure, and become solid particles which would be transported through the steam into the turbine components.

From sample 0 to sample 1, it is observed that the average C content is consumed, while the average content for Cr, O, Na, and Nb is increased.

Table 6. Chemical composition after cyclic oxidation in air. Sample 1.

Element	**Concentration**								
	Spot 1	**Spot 2**	**Spot 3**	**Spot 4**	**Spot 5**	**Spot 6**	**Spot 7**	**Spot 8**	**Spot 9**
Carbon (C)	0.2	0	0	0.1	0	0	0	0	0
Iron (Fe)	4.5	18	5.4	14.8	3.7	8.3	6.4	1.7	1.4
Chromium	4.2	14.6	20.7	23.5	22.9	22.5	27.4	25.7	20.4
Oxygen (O)	55.9	51.6	65.7	43.9	67.1	62.8	60.5	67.9	38.9
Nickel (Ni)		6.8		6.7					0.3
Nitrogen (N)			1.8		1.9	1.6	1.8	1.7	
Silicon (Si)	2.6	5.2	0.7	1.7	0.9	1.6	0.7	0.6	0.3
Niobium	0.2	1.2	0.2	0.6	0.7	1	0.8	0.6	0.5
Alluminium	29.4								
Manganese (Mn)	0.6	2.7	1.6	3.2	2.8	2.3	2.3	1.8	2
Sulphur (S)	0.9			1.6					8.2
Sodium (Na)				3.9					28
Calcium (Ca)	1.5								
Zinc (Zn)			3.9						
TOTAL	**100**	**100.1**	**100**	**100**	**100**	**100.1**	**99.9**	**100**	**100**

Fe, Ni, N, and Si content has been decreased, and finally elements like Cl, K and Mo are completely depleted.

New elements such as S, Ca and Zn appear as a result of the oxidation.

Al and Cr will ultimately form the protective oxide layer on the substrate, as anticipated at the beginning of the project.

5.3.3 Sample 2. SEM and EDS.

Hot corrosion in the presence of molten Na_2SO_4 salt (sample 1), resulted in the formation of micro-crystals as observed on the surface of the sample 2, in figure 15.

A surface similar to that of sample 0 is observed under the micro-crystals, without the layers resulted from spallation as in sample 1.

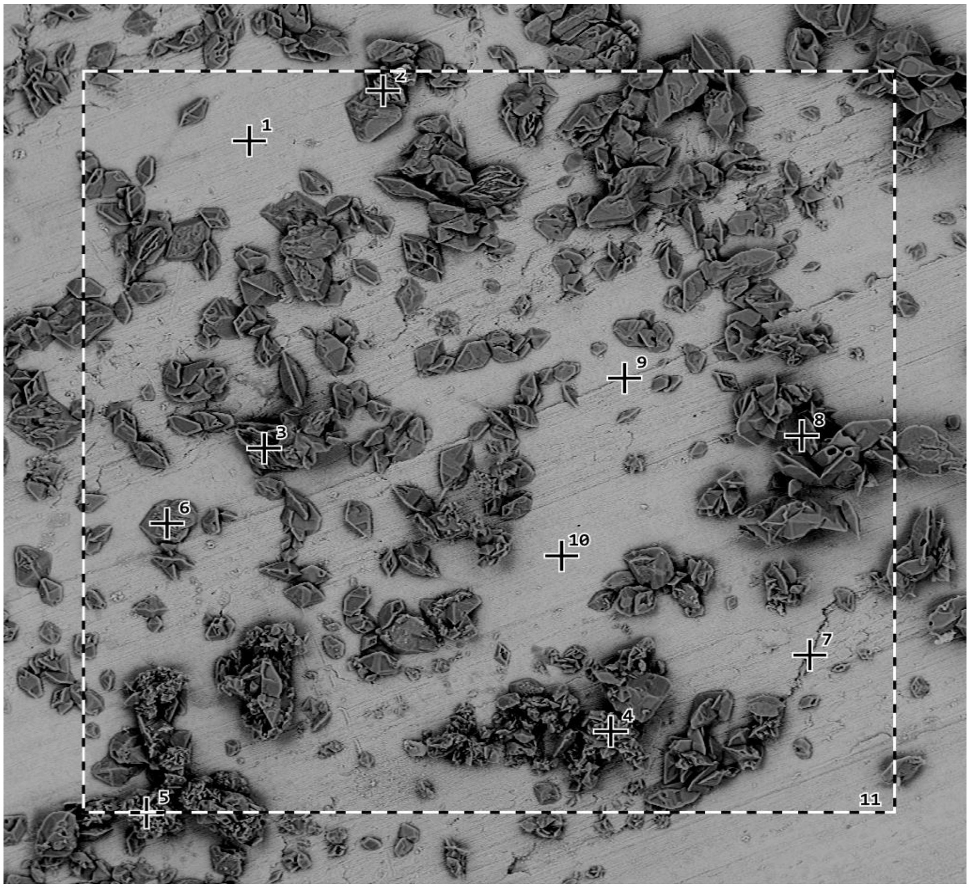

Figure 15. Sample 2, surface morphology.

The crystals resulting from molten salt plus the metallic substrate, constitute the hot corrosion product of this particular sample. This is proven by looking at the chemical composition on spot 6 on table 7, where apart from other chemical elements, sodium (Na) and sulphur (S) are also present.

The average carbon (C) content is consumed, while element content of Fe, Cr, Ni and Si are decreased.

Table 7. Chemical composition after hot corrosion in Na_2SO_4. Sample 2.

Element	Concentration								
	Spot 1	**Spot 2**	**Spot 3**	**Spot 4**	**Spot 5**	**Spot 6**	**Spot 7**	**Spot 8**	**Spot 9**
Carbon (C)	0	0	0.3	0	0.1	0.2	0.1	0	0
Iron (Fe)	9.7	0.4	5.1	0.6	0.9	1.4	29.7	26.4	10.1
Chromium (Cr)	15.7	1.4	24.3	1.4	1.2	5.9	24.8	17.5	13.1
Oxygen (O)	48.9	45.6	28.8	43	46.1	33.4	9.2	12.8	52.3
Nickel (Ni)	8.2	0.3	3.6	0.4	0.5	0.7	24.4	20.9	6.9
Silicon (Si)	4.7	0.3	0.5	0.3	0.2	0.6	1.1	0.8	2.2
Sodium (Na)	3.3	39.8	13.5	34.7	35.2	28.6	5.5	15.4	10.9
Niobium (Nb)	3.9	0.9	1.4	1.4	0.9	1.8	1.3	0.6	0.7
Manganese (Mn)	5.1	0.3	4.3	0.3	0.4	1.7	3.2	3.1	3.1
Sulphur (S)	0.4	11.2	18.2	17.9	14.5	25.7	0.6	2.6	0.6
TOTAL	**99.9**	**100.2**	**100**	**100**	**100**	**100**	**99.9**	**100.1**	**99.9**

Average content of O, Na, and Nb show an increase. Elements like Cl, K, Mo, and Al are completely depleted.

The depletion of aluminum and the decrease is chromium suggests the formation of a protective oxide.

Finally, this section has examined the surface morphology changes observed on the samples, before and after cyclic oxidation and hot corrosion processes took place. Each sample adopted a different morphology and slightly different chemical composition, since the exposure conditions differed.

Figure 14 compares the surface morphologies observed under the microscope. Sample 3 was not displayed due to technical difficulties.

5.4 PROJECT LIMITATIONS

The third objective of this project, which consisted n characterizing the chemical composition of the corrosion product could not be attained given that the XRD machine in Universiti Teknologi Petronas was broken.

Additionally, the SEM was unable to read sample 3, this is the reason why this sample's morphology and chemical composition is not reflected in this report.

The execution of the experiment in a laboratory also constitute a major limitation of this project, because a thermal power plant or an incinerator plant condition would have provided the ideal combustion and corrosive environments, and better mimic the real operating scenario faced by the metallic alloy.

Finally, given the unavailability of the laboratory technician in charge, SEM were not run on the cross-sectional surfaces of the samples.

CHAPTER 6
CONCLUSION AND RECOMMENDATION

6.1 Conclusion

The characterization of the boiler tube steels at high temperatures is the main objective of this research project.

This study focuses on the analysis of the composition of the metallic alloy, and how the adverse temperature conditions, and corrosive environments affect the physical, mechanical and chemical integrity of the steel.

An experiment was carried on consisting of exposing three samples of the same metallic alloy, to different corrosive conditions, at a temperature of 700^{o}C, in a laboratory furnace. These samples were subjected to either oxidation or hot corrosion, sample 1 and samples 2 and 3, respectively. It was observed that, sample 1 exposed to cyclic oxidation in air presented spallation, which consists in the fragmentation of the metallic substrate into thin layers; with a continuous exposure as it would occur in an actual boiler, these layers will further break into micro solid particles, which are in turn driven downstream with the steam, into the turbine components, causing erosion and wear at these points.

The chemical composition on sample 1 surface, after cyclic oxidation revealed a drastic consumption of carbon, while the iron, nickel and silicon contents appear to have been decreased. Sample 2 on the other hand, presented a surface morphology covered with micro-crystals. The carbon content is consumed almost to zero, and elements such as Fe, Si. Cr and Nickel decrease in content significantly. Given the sodium sulphate coating solution, Na and S appear on the surface of this sample.

Finally, the predicted behavior of the oxidation and hot corrosion processes has been visualized in this project. The characterization of the chemical composition before and after the processes has also been accomplished, and the identification of the most relevant corrosion-contributing elements would have been determined, with the air of an Xray diffraction analysis, which was not possible in this project time scope, since the machine was unavailable.

6.2 Recommendation

It is recommended to run the SEM/EDS analysis on the cross-sectional surfaces, in order to determine the depth of penetration of the processes of oxidation and hot corrosion, in each sample. In this manner, it is possible to better characterize the oxidation and hot corrosion resistance of the steel KHR35C.

The Xray Diffraction analysis is as well recommended for the complete fulfillment of this project, since characterization of the corrosion products is not possible without this tool.

REFERENCES

[1] Kapooria, R., Kumar, S., Kasar, K. (2008). An analysis of a termal power plant working on a Rankine Cycle: A theoretical investigation. [Online]. Aavailable: http://www.erc.uct.ac.za/jesa/volume19/19-1jesa-kapooria-etal.pdf

[2] Kumar, R., Tewari, V., Prakash, S.(2007). Studies on Hot Corrosion of the 2.25 Cr-1Mo Boiler Tube Steel and Its Weldments in the Molten Salt Na2SO4-60 pct V2O5 Environment. *Metallurgical and Materials Transactions A*. Vol 38A, 54-57. Doi: 10.1007/s11661-006-9053-x

[3] Pollock, T.,Tin,S. (2006). Nickel-Based Superalloys for Advanced Turbine Engines: Chemistry, Microstructure, and Properties. *Journal of Propulsion and Power*, Vol. 22, No. 2, (361-374)

[4] Stringer, J. (1993). "High temperature corrosion in practical systems." Le Journal de Physique IV **03**(C9): C9-43-C49-61.

[5] Meier, G. H., Pettit, F. S. (1999) "Oxidation and hot corrosion of superalloys." *Metallurgical and Materials Engineering Department*. University of Pittsburgh.

[6] Kamal, S., Prakash, S. (2010). "High Temperature Cyclic Oxidation and Hot Corrosion Behaviour of Superalloys at 900oC." *Department of Metallurgical and Material Engineering*. Indian Institute of Technology. (Page 299).

[7] Kamal, S., Kumar, C.,& Singh, A. (2012). Hot Corrosion Behavior of Detonation Gun Sprayed 75Cr3C2-25(80Ni-20Cr) Coating in Molten Salt Environment. School of Engineering & Technology. University of Sharda. *International Journal of Engineering Research & Technology*. Vol. 1 Issue 9

[8] Themal Spray Coating Processes. Retrieved from http://www.tstcoatings.com/thermal_spray_processes.html, on August 10th, 2014.

[9] Kamal, S., Jayaganthan, R., & Prakash, S. (2010). Hot Corrosion Studies of Detonation-Gun-Sprayed NiCrAlY + 0.4 wt.% CeO2 Coated Superalloys in Molten Salt Environment. *Journal of Materials Engineering and Performance, 20*(6), 1068-1077. doi: 10.1007/s11665-010-9728-8

APPENDICES

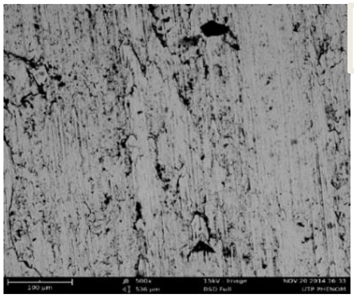

SAMPLE 0

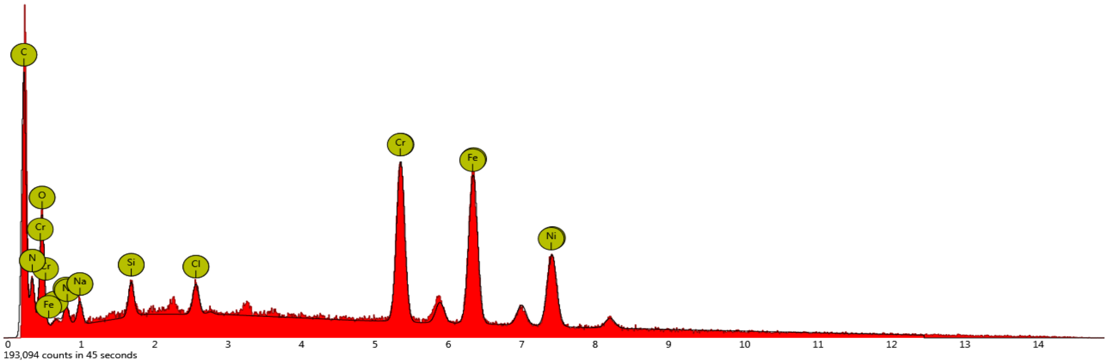

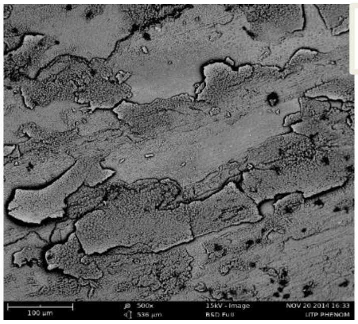

SAMPLE 1

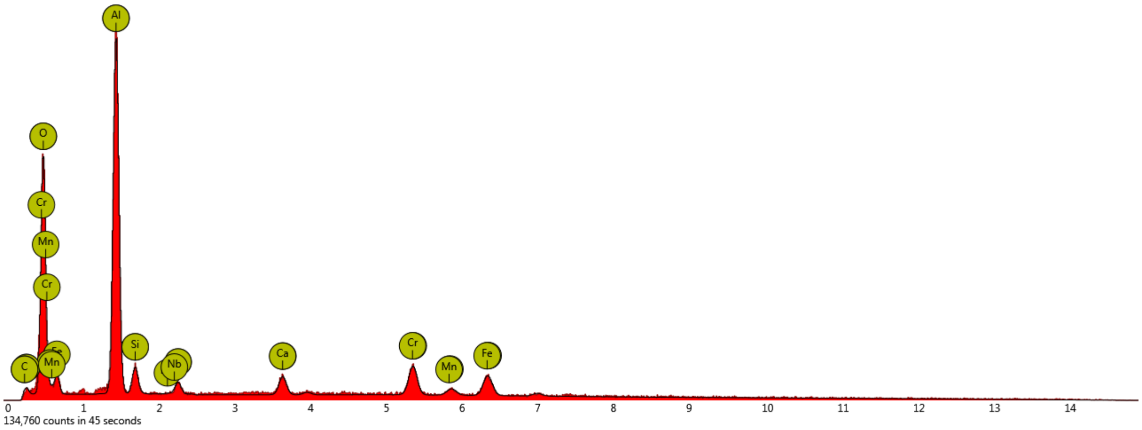

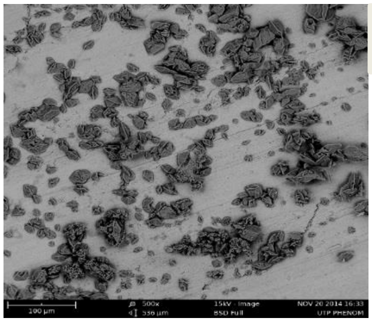

SAMPLE 2

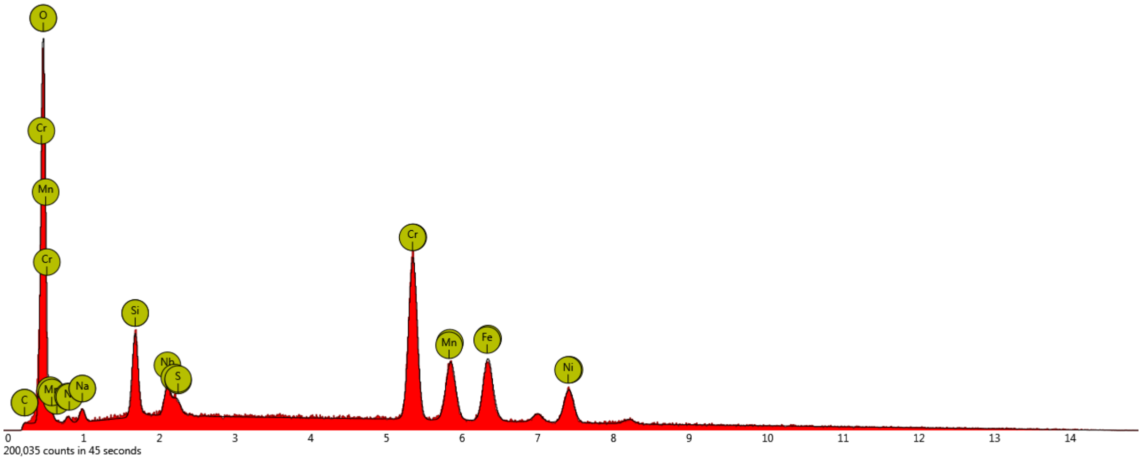

Appendix I. Microscopic view of the surface morphologies of the samples tested.